Dalton Transactions

PAPER

View Article Online
View Journal | View Issue

Cite this: *Dalton Trans.*, 2014, **43**, 1577

Photocurrent enhanced dye-sensitized solar cells based on TiO_2 loaded $K_6SiW_{11}O_{39}Co(II)(H_2O)\cdot xH_2O$ photoanode materials†

Liang Li,[a] YuLin Yang,*[a] RuiQing Fan,*[a] Xin Wang,[a] Qingming Zhang,[a] Lingyun Zhang,[a] Bin Yang,[b] Wenwu Cao,*[b,c] Wenzhi Zhang,[d] Yazhen Wang[d] and Liqun Ma[d]

Received 12th August 2013,
Accepted 8th October 2013

DOI: 10.1039/c3dt52201f

www.rsc.org/dalton

Through loading of TiO_2 on the surface of $K_6SiW_{11}O_{39}Co(II)(H_2O)\cdot xH_2O$ ($SiW_{11}Co$), a novel photoanode material has been created for dye-sensitized solar cells (DSSC). The absorbing band as well as photoelectricity response range of TiO_2@$SiW_{11}Co$ is extended to the visible range. In addition, the absorption in the UV range is enhanced notably compared with P25 (raw TiO_2). More importantly, the recombination of the TiO_2 network is avoided. TiO_2@$SiW_{11}Co$ is mixed with P25 powder (wt ~1 : 1) to assemble dye-sensitized (N719) solar cells, which exhibit a short-circuit photocurrent density as high as 18.05 mA cm^{-2}, which is 64% higher than blank samples under the standard AM1.5G global solar irradiation. In addition, the mechanisms for $SiW_{11}Co$ in DSSC are proposed.

1. Introduction

Direct utilization of solar radiation to produce electricity is an ideal way to utilize nature's renewable energy. Dye-sensitized solar cells (DSSCs) are one of the most promising solutions with low cost, nontoxicity and long-term stability. DSSCs are structured like a sandwich with a photoanode, a photocathode and a drop of electrolyte. Semiconductor photoanodes have been studied for over twenty years.[1] Among them, TiO_2 and ZnO are the most widely used photoanode materials.[2] Because of the narrow absorbing range of the sunlight spectrum of TiO_2 (λ < 380 nm), dyes or inorganic quantum dots are used to absorb visible light to sensitize the semiconductor. N719 is a red dye which is usually used as a standard to evaluate the performance of DSSCs. However, N719 can only absorb the visible light from 400 nm to 700 nm[3] which limits the overlap with the solar spectrum. Using co-sensitizers which operate in different regions of the solar spectrum is one approach for broad spectral coverage of the photoresponse.[4] TiO_2 with tunable band gap is also used to enhance the light absorption of DSSCs.[5,6] N-doping can narrow the band gap of TiO_2 to a certain extent, and make it easier to accept the electrons from the sensitizer.[7] Recently, heteropolyacids (HPAs) have been widely employed as catalysts[8,9] in heterogeneous reactions due to their unique structural and chemical properties, and it is expected to decrease fast electron–hole recombination on TiO_2 due to their long transient lifetime. Also, they are known to be ionic solids based on high molecular weight anions having the general formula $[X_xM_nO_y]^{3-}$ with $x \leq n$ and may enhance ionic transport across dye-sensitized solar cells.[10] $H_3PW_{12}O_{40}$-doped TiO_2 has been briefly reported in a communication, and it was found that the electron lifetime become longer following an increase in the amount of the polyoxometalate with a 9.43% enhanced photocurrent.[11] Differently, in this study, we attempted to load TiO_2 onto the surface of red $K_6SiW_{11}O_{39}Co(II)(H_2O)\cdot xH_2O$ ($SiW_{11}Co$) by using a simple one-step reaction, that exhibits a short-circuit photocurrent density as high as 18.05 mA cm^{-2}, which is 64% higher than blank samples under the standard AM1.5G global solar irradiation. Also, through summarizing the previous literature and the test data we have, a working mechanism for $SiW_{11}Co$ in DSSCs is proposed.

[a]*Department of Applied Chemistry, Harbin Institute of Technology, Harbin, China. E-mail: ylyang@hit.edu.cn, fanruiqing@hit.edu.cn; Fax: +86 451 86418270; Tel: +86 451 86413710*

[b]*Condensed Matter Science and Technology Institute, Harbin Institute of Technology, Harbin 150001, China*

[c]*Materials Research Institute, The Pennsylvania State University, University Park, Pennsylvania 16802, USA. E-mail: dzk@psu.edu; Fax: +1 814 8652326; Tel: +1 814 8654101*

[d]*College of Chemistry and Chemical Engineering, Qiqihar University, Qiqihar 161006, Heilongjiang Province, PR China*

†Electronic supplementary information (ESI) available: FT-IR spectrum of $K_6SiW_{11}O_{39}Co(II)$, transmittance, XRD and EDS of TiO_2@$SiW_{11}Co$. See DOI: 10.1039/c3dt52201f

2. Experimental

2.1. Materials and reagents

$K_4[Si(W_3O_{10})_4]\cdot xH_2O$, cobalt acetate, acetone, isopropyl titanate, *n*-butyl alcohol, absolute ethyl alcohol, I_2, LiI, *tert*-butylpyridine (TBP), acetonitrile, propylene carbonate, *cis*-bis(isothiocyanato)bis(2,2-bipyridyl-4,4-dicarboxylato)ruthenium(II) bis-tetrabutylammonium (N719), F-doped SnO_2-coated glass plate (FTO, 90% transmittance in the visible, 15 Ω cm^{-2}).

2.2. Fabrication of $SiW_{11}Co$ and TiO_2@$SiW_{11}Co$

$SiW_{11}Co$ was synthesized using a similar method as that discussed in the literature.[12] $K_4[Si(W_3O_{10})_4]\cdot xH_2O$ (2.0 mmol) was dissolved into 30 mL distilled water in a flask and then heated at 95 °C in a water bath with constant stirring. A saturated solution of cobalt acetate (2.2 mmol) was added into the flask dropwise, and then left to stand for an hour. After evaporating the reaction solution to about 10 mL, and cooling it down to room temperature, 30 mL acetone was added and the precipitate was filtered. The last step was repeated until there was no more precipitate, and the solution was transferred into a vacuum oven at 50 °C to obtain red block crystals. The ICP analysis showed that the prepared $SiW_{11}Co$ has the atomic ratio Si : W : Co : K ~ 1 : 10.90 : 1.02 : 5.94 (calcd: 1 : 11 : 1 : 6). According to the FT-IR spectrum (Fig. S1†), the characteristic stretching vibrations for $SiW_{11}Co$ were observed at 964 cm^{-1} (W–O_d), 906 cm^{-1} (Si–O_a), 814 cm^{-1} (W–O_b–W) and 741 cm^{-1} (W–O_c–W).[13] The peak at 533 cm^{-1} confirmed the Keggin structure of $SiW_{11}Co$ to be the same as that reported the literature.[13]

The TiO_2-loaded $SiW_{11}Co$ used as photoanode material was synthesized as follows: 0.05 g $SiW_{11}Co$ was dissolved in distilled water by stirring it to form a dark red stock solution. Concurrently, 5 mL isopropyl titanate was dropwise added into 3 mL *n*-butyl alcohol. As soon as the two solutions were clarified, the solution of $SiW_{11}Co$ was added dropwise into the solution of isopropyl titanate with stirring. Then, the turbid solution was heated at 45 °C for 3 h and at 80 °C for about 3 h until a hydrogel formed. The hydrogel was transferred into a 45 °C vacuum oven and maintained for 12 hours and then at 80 °C for 3 more hours. After washing 3–5 times by distilled water, it was dried at 80 °C for 3 hours. Finally, TiO_2-loaded $SiW_{11}Co$ was obtained after calcining at 450 °C.

2.3. Characterization

Scanning electron microscopy (SEM) micrographs were taken using a Hitachi S4800 instrument operating at 15 kV. Fourier transform (FT)-IR spectra were measured on a Perkin-Elmer Spectrum 100 FT-IR spectrometer with samples prepared as KBr pellets. The SPS instrument was assembled by Jilin University. Monochromatic light was obtained by passing light from a 500 W xenon lamp through a double-prism monochromator (SBP300, China), and the signal was collected by a lock-in amplifier (SR830, Stanford). UV-vis spectra were taken by a UV-3600 (Shimadzu, Japan). Electrochemical impedance spectra were recorded by a CHI660D Electrochemical Analyzer (Chenhua, China). The sample was sandwiched between two FTO glass electrodes. Optically transparent electrodes were made from an F-doped SnO_2-coated glass plate purchased from Acros Organics, Belgium. The films were immersed in a 0.3 mM N719 (Solaronix SA, Switzerland) in absolute ethyl alcohol for 24 h at room temperature. The electrolyte composed of 0.05 M I_2, 0.5 M LiI, and 0.1 M TBP in 1 : 1 (volume ratio) acetonitrile–propylene carbonate was admitted by capillary action. Photocurrent–photovoltage curves were recorded by a CHI660D electrochemical analyzer. The light intensity of AM1.5 global sunlight from a filtered 500 W xenon lamp (CHF-XM500, Changtuo, China with an AM1.5 global filter from Newport) was calibrated by a standard Si solar cell (calibrated at National Institute of Metrology, P. R. China). The incident photon to current efficiency (IPCE) was measured on an EQE/IPCE spectral response system (Newport). All characterizations were carried out under ambient pressure and temperature.

3. Results and discussion

Fig. 1 shows the SEM images of $SiW_{11}Co$ before and after loading with TiO_2. $SiW_{11}Co$ has a lamellar structure with some small surfaces. After loading with TiO_2 and calcining at 450 °C, TiO_2@$SiW_{11}Co$ changed into small pieces coated by TiO_2 particles. Also the smooth surface became rough. According to the XRD pattern of TiO_2@$SiW_{11}Co$ (Fig. S2†), the phase can be confirmed as anatase.

Fig. 2 shows the UV-vis absorption of TiO_2@$SiW_{11}Co$ compared with blank samples of pure $SiW_{11}Co$ and commercial P25. For both pure $SiW_{11}Co$ and TiO_2@$SiW_{11}Co$, an absorption ranging from 300 nm to 700 nm is observed. As reported in the literature, TiO_2 only absorbs UV light (λ < 387 nm) without any absorption in the visible and infrared regions.[7] However, it shows a good visible absorption when TiO_2 is loaded onto the

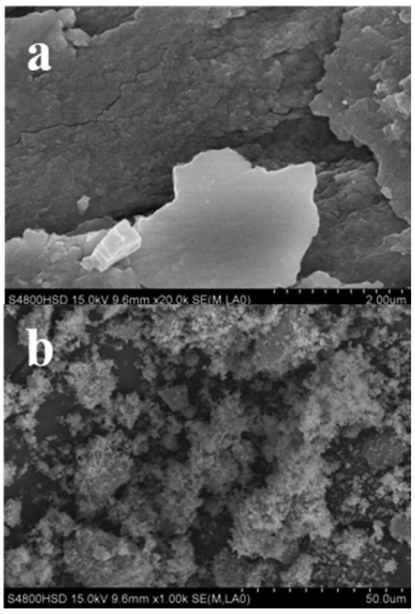

Fig. 1 SEM images of $SiW_{11}Co$ (a) and TiO_2@$SiW_{11}Co$ (b).

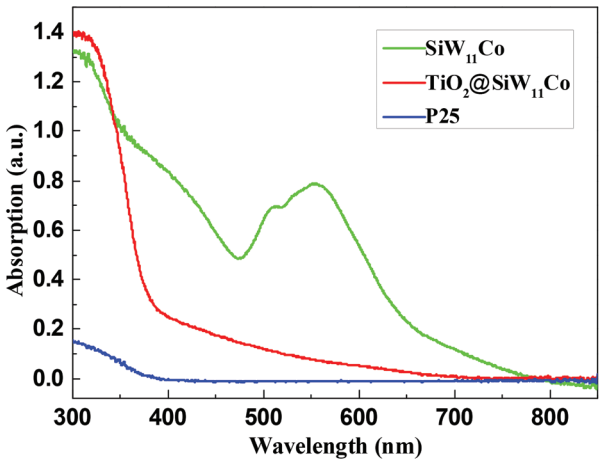

Fig. 2 UV-vis spectra of $SiW_{11}Co$, commercial P25 and TiO_2@$SiW_{11}Co$.

surface of $SiW_{11}Co$. In addition, a transmittance spectra is presented in the ESI as Fig. S3† along with the analysis.

The surface photovoltage spectrum (SPS) as a well-established noncontact and nondestructive technique can offer important information about the semiconductor surface, interface and bulk properties, and reflects the photogenerated charge separation and transfer behavior with the aid of light.[14–16] Fig. 3 displays the SPS spectra of pristine P25 and TiO_2@$SiW_{11}Co$ powders without external bias. In the UV region, it is clear that both spectra have similar profiles. The positive peak in the wavelength range from 300 to 400 nm for pure TiO_2 was attributed to the transition O 2p–Ti 3d.[17] So TiO_2 on the surface of $SiW_{11}Co$ maintained the properties of pure TiO_2. In the visible region, the SPS signal of TiO_2@$SiW_{11}Co$ was enhanced significantly compared with P25 (Fig. 3), which shows that after introducing $SiW_{11}Co$, the light response region of the sample was extended to the visible band.

The TiO_2@$SiW_{11}Co$ were screen-printed and sensitized as dyed photoanode, and the SPS spectra of the dyed photoanode were measured to investigate the properties of the new photoanode in a DSSC (see Fig. 4). The thickness of the coating film was controlled in screen printing. Therefore, for the film thickness, and the same illumination coverage, the SPS intensity

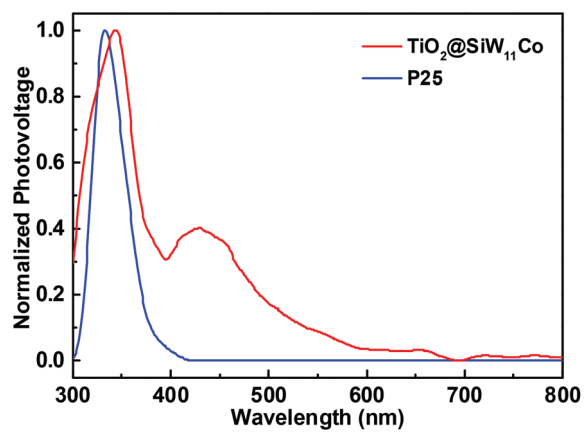

Fig. 3 Normalized SPS of P25 and TiO_2@$SiW_{11}Co$.

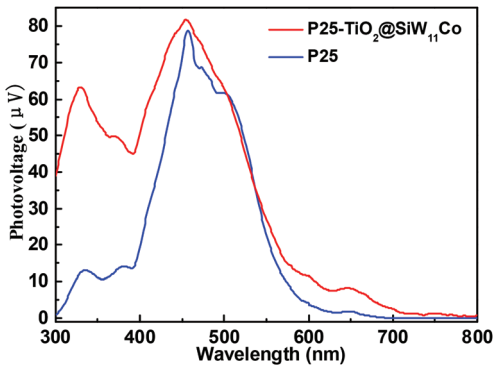

Fig. 4 SPS of N719 sensitized photoanode with P25 and TiO_2@$SiW_{11}Co$.

can be quantitatively characterized and compared. In general, higher SPS signal suggests a larger difference in band bending before and after light irradiation. The SPS intensity in the UV region increased after TiO_2 was loaded on $SiW_{11}Co$. The difference in band bending is caused by the accumulation of photogenerated electrons on the surface, which are static electrons. Larger SPS signal means a greater number of static electrons accumulated on the surface. In the visible region, it shows no weaker photoelectric signal than P25. Even a combined signal of N719 and $SiW_{11}Co$ can be observed obviously in Fig. 4. Accordingly, $SiW_{11}Co$ can assist TiO_2 to generate a stronger SPS signal. For a given photoanode material, the surface properties could significantly affect the photoelectrochemistry activity. The UV-visible absorption spectroscopy and SPS demonstrates that the new photoelectrode of FTO/P25–TiO_2@$SiW_{11}Co$ possessed favorable optical and photovoltaic properties.

To acquire a better perspective on the sensitized enhancement mechanism of the photoelectrode heterostructure, the photogenerated electron transfer process between interfaces of $SiW_{11}Co$ and TiO_2 have been studied, and a fabricated structure similar to the standard configuration of dye-sensitized solar cells is given in Fig. 5. Upon excitation by the sunlight, the N719 molecules absorb the visible light (from 400 nm to 700 nm) and reach their excited state (Dye*). Concurrently, TiO_2@$SiW_{11}Co$ particles (mainly $SiW_{11}Co$ coated by TiO_2) absorb the visible light, and inject electrons into the *n*-TiO_2 nanoparticles network, which were composed of TiO_2 on the

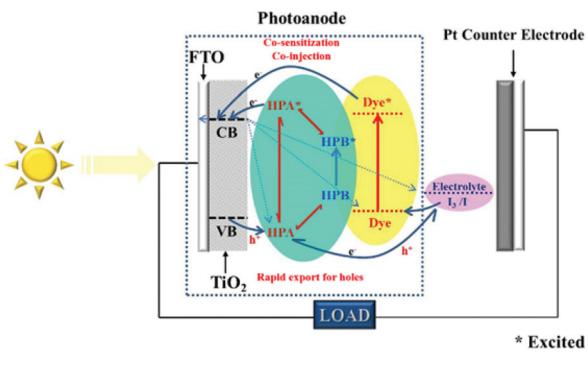

Fig. 5 Schematic illustration of the dye-sensitized photovoltaic cell [FTO/P25–TiO_2@$SiW_{11}Co$/dye/electrolyte/Pt/FTO].

surface of $SiW_{11}Co$ as well as P25, similarly to N719. Holes in TiO_2 were conducted out by $SiW_{11}Co$ and then injected to the electrolyte. However, a certain amount of excited electrons return back to the ground state of the dye and some react with iodine in the electrolyte (dotted lines in Fig. 5), particularly at the interfacial region, which may be overcome by introducing a powerful electron acceptor. HPB (heteropolyblue) cannot be ignored considering the reducibility of I^- ions. Also, in sunlight, most injected electrons are recaptured by I_3^- before being extracted to the external circuit. $SiW_{11}Co$ captured the returning electrons to reduce itself to form HPB. HPB in this process plays a similar role to $SiW_{11}Co$, absorbing light and injecting electrons. Meanwhile, the oxidized dye and $SiW_{11}Co$ is regenerated by I^-. As a result, the absorbed photon energy is converted to heat through the two coupled redox cycles involving sensitized electron injection, dye regeneration, and electron recapture by I_3^-. The counter electrode is kept at equilibrium, because there is no net current flowing through it. In general, introducing $SiW_{11}Co$ can avoid most of the backward reactions that take place in standard dye-sensitized solar cell systems which reduces the power conversion efficiency (PCE).

On the other hand, under light illumination, another process may take place in the $SiW_{11}Co$ system: O → M CT (charge transfer); the band of $SiW_{11}Co$ was excited by the illumination, which resulted in electron–hole separation.[18] Excited $SiW_{11}Co$ injects electrons into the conduction band of TiO_2 and the electron holes in the valence band were conducted out rapidly. The intermediate HPB was excited and returned back to the excited $SiW_{11}Co$, which subsequently returned to the ground state of $SiW_{11}Co$.[19] Thus, it avoided the photoreduction of iodine on the surface of the photoanode. Such an effective electron transfer in $SiW_{11}Co$ can remove the fast electron–hole recombination on TiO_2 and is ascertained from the lifetime of the transient species available in the literature.[19] In addition, high charge separation created within $SiW_{11}Co$ avoids further electron–hole recombination. As a result, the high surface area and good hole-mobility of the TiO_2@$SiW_{11}Co$ contribute favorably for the photocurrent generation by enhancing the absorption and avoiding the regeneration of electrode. Furthermore, it increases the mobility of electrons, which reduce the chance for electron–hole recombination. All these effects greatly improved the performance and stability of fabricated solar cells.

Typical EIS data obtained for both devices based on P25 and P25/TiO_2@$SiW_{11}Co$ under illumination at a bias voltage corresponding to the V_{oc} are presented in Fig. 6. The first arc in the high frequency range of the Nyquist plot (Fig. 6a) is assigned to the electron-transfer process at the EL–CE interface. A linear Warburg impedance feature appears in the middle frequency range. This arises from the increase in the electron-transport resistance of the TiO_2 film due to the decrease of the electron concentration, upon lowering the forward bias. In the corresponding Bode plot (Fig. 6b), the phase angle peak, corresponding to the electron diffusion time constant in the photoanode film, appears in the middle frequency range (from 100 to 1000 Hz). Utilizing TiO_2@

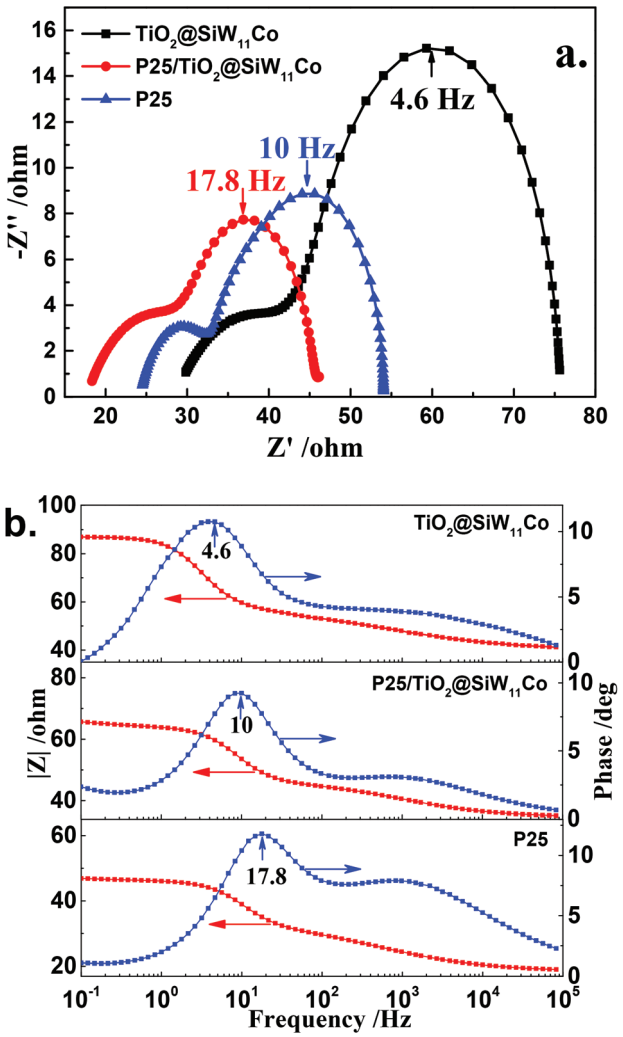

Fig. 6 EIS of DSSCs with P25 and P25–TiO_2@$SiW_{11}Co$: (a) Nyquist plot; (b) Bode plot of P25, TiO_2@$SiW_{11}Co$ and P25–TiO_2@$SiW_{11}Co$.

$SiW_{11}Co$ as a photoanode material with an increase of the radius of the semicircle in the Nyquist plot (see Fig. 6a) indicates a reduction in the interfacial charge recombination rate. In accordance with this observation, the corresponding phase angle peak in the Bode plot (Fig. 6b) located in the low frequency shifts to a lower frequency (from 17.8 Hz to 4.6 Hz). This indicates a longer electron lifetime for DSSC with P25/TiO_2@$SiW_{11}Co$.[20] From the Bode phase plots, the electron lifetime with TiO_2@$SiW_{11}Co$ is much longer than that obtained with commercial P25 at the same light intensity. However, the impedance of DSSC with TiO_2@$SiW_{11}Co$ is too large to present an excellent performance. Thus, mixing with commercial P25 powder is a good method to balance the large impedance and the long electron lifetime. Fig. 6 shows the Nyquist plot and Bode plot of DSSC with P25 and TiO_2@$SiW_{11}Co$, and both the impedance and the electron lifetime stand between P25 and TiO_2@$SiW_{11}Co$, which demonstrates an excellent performance.

These electronic processes in the DSSCs are well described by the transmission line model shown in Fig. 7. The equivalent

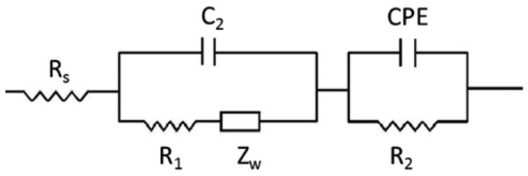

Fig. 7 Equivalent circuit used to fit the impedance measurements on the DSSCs.

circuit elements have the following meanings: the symbols R and C describe resistance and capacitance, respectively; O accounts for a finite-length Warburg diffusion (Z_{Diff}), which depends on the parameters $Y_{o,1}$ and B, and Q is the symbol for the constant phase element, CPE (its parameters are $Y_{o,2}$ and n).[21] Table 1 lists parameters obtained by fitting the impedance spectra of composite solar cells using the equivalent circuit. The series resistance of the system (R_s) can account for the resistance of the electrolyte, the resistance within the photoelectrode film and the FTO electrode, as well as the contact resistance. A short straight line observed at high frequency is associated with the capacitance and resistance at Pt–electrolyte interface (CPE and R_2 elements).[21] For the parameters related to the Pt–electrolyte interface, R_2 deceased from 15.1 to 11.87 ohm by using TiO_2@$SiW_{11}Co$, so that much more I_3^- on the Pt electrode surface can form through redox reactions.[9] However, the DSSC with TiO_2@$SiW_{11}Co$ shows an R_s value of 29.83 ohm, R_1 value of 20.33 ohm and R_2 value of 17.24 ohm, which are larger than both that of P25 and P25–TiO_2@$SiW_{11}Co$. This indicates that the impedance of the photoanode film is too large to achieve a satisfactory performance. The large semicircle at medium frequency was attributed to the electron transfer process at the dyed-photoanode-material–electrolyte interface (capacitance, C_1; charge transfer resistance, R_1).[21,22] C_1 decreased from 1.161 to 0.994 mF and R_1 increased from 12.97 to 17.05 Ω by loading TiO_2 on $SiW_{11}Co$; the increasing value of R_1 means that the recombination resistance is high at the dyed-TiO_2@$SiW_{11}Co$–electrolyte interface. Correspondingly, the value of C_1 decreased slightly, so that the electrons at the dyed-TiO_2@$SiW_{11}Co$–electrolyte interface remain the same as that of the DSSC using P25 (~86%) electrodes. The high recombination resistance and similar film capacitance are favorable for improving the performances of DSSC.[23]

Incident photon-to-electron conversion efficiency (IPCE) curves are shown in Fig. 8. For the blank DSSC with P25, it showed a standard IPCE curve similar to that reported in the literature.[24] The IPCE value peaked at around 540 nm, which is consistent with the UV-vis absorption maximum. From the IPCE curve of DSSCs with P25 and TiO_2@$SiW_{11}Co$, one can see

Table 1 Summary of parameters of the equivalent circuit

DSSC samples	R_s/Ω	C_1/μF	R_1/Ω	R_2/Ω
P25	18.33	1161	12.97	15.1
P25-TiO_2/$SiW_{11}Co$	24.53	994.4	17.05	11.87
TiO_2/$SiW_{11}Co$	29.83	621.5	20.33	17.24

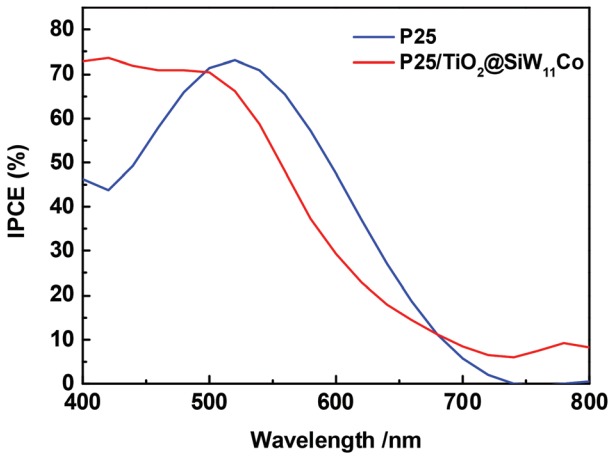

Fig. 8 The incident photon-to-current efficiency (IPCE) of dye-sensitized solar cells based on P25, TiO_2@$SiW_{11}Co$ and P25–TiO_2@$SiW_{11}Co$.

a significant enhancement in the high-energy blue region as shown in Fig. 8. In the spectrum, the photocurrent contribution from $SiW_{11}Co$ and N719 are generated from λ = 400 to beyond 510 nm, and from 450 to beyond 600 nm, respectively. Through loading TiO_2 on the surface of $SiW_{11}Co$, the IPCE from 400 to 500 nm drastically increased from 45% to 72%. A region of $SiW_{11}Co$ was introduced into the absorption and photon–electron curve. Besides, the region of N719 maintained a good IPCE value, only about 10% lower than that of the blank DSSC. As a result, the DSSC based on P25 and TiO_2@$SiW_{11}Co$ showed a much improved performance.

Fig. 9 shows the current density–voltage curves of DSSCs based on films of a mixture of P25 and TiO_2@$SiW_{11}Co$ under 100 mW cm^{-2} illumination. The corresponding photovoltaic data are summarized in Table 2 with very good reproducibility. Based on the J–V curve, the fill factor (FF) is defined as:

$$FF = (J_{max} \times V_{max})/(J_{sc} \times V_{oc}) \quad (1)$$

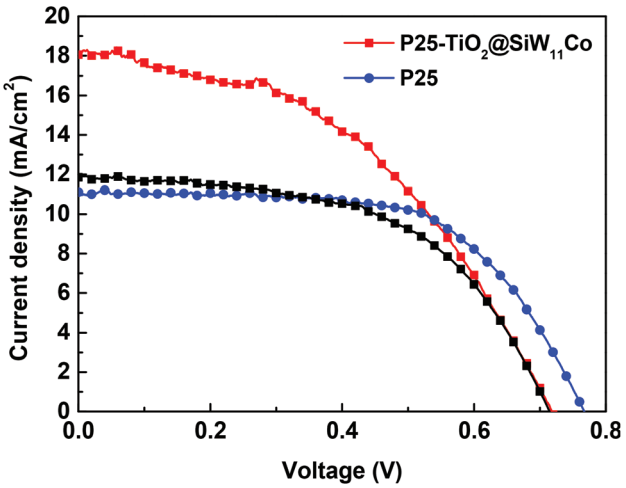

Fig. 9 The current density *versus* voltage curves of dye-sensitized solar cells based on P25, TiO_2@$SiW_{11}Co$ and P25–TiO_2@$SiW_{11}Co$ under 100 mW cm^{-2} illumination.

Table 2 Comparison of J–V performance of TiO_2@$SiW_{11}Co$, P25–TiO_2@ $SiW_{11}Co$ and P25 (raw TiO_2) photoelectrodes

DSSC devices	J_{sc} (mA cm^{-2})	V_{oc} (V)	FF	PCE (%)
P25	11.01	0.771	0.62	5.2
TiO_2/$SiW_{11}Co$	11.86	0.714	0.55	4.6
P25–TiO_2/$SiW_{11}Co$	18.05	0.718	0.46	6.0

where J_{max} and V_{max} are the photocurrent density and photovoltage for maximum power output, and J_{sc} and V_{oc} are the short-circuit photocurrent density and open-circuit photovoltage, respectively. PCE is the overall power conversion efficiency (P_{in} is the power of incident light which is 100 mW cm^{-2} in this work), defined as

$$\mathrm{PCE} = (\mathrm{FF} \times J_{sc} \times V_{oc})/P_{in} \quad (2)$$

When applied in a DSSC alone without P25, TiO_2@$SiW_{11}Co$ shows a J_{sc} value of 11.86 mA cm^{-2}, which is slightly higher than P25. However, due to a lower FF value, the PCE value is only 4.6%, which is much lower than P25. However, when mixing TiO_2@$SiW_{11}Co$ powder and P25 in the weight ratio of 1 : 1, an enhanced performance was achieved. Compared with the DSSC based on P25, DSSCs with TiO_2@$SiW_{11}Co$ exhibit better performance. J_{sc} values increased to 18.05 mA cm^{-2}, which was 164% of that of the DSSC based on P25. The V_{oc} decreased from 0.771 V to 0.718 V, which changed little compared with the DSSC with P25 alone. In general, a 6.0% PCE was achieved due to the low fill factor.

4. Conclusions

In summary, we have successfully synthesized a novel photoanode material, TiO_2@$SiW_{11}Co$, and used it for the first time to fabricate a DSSC with high performance. TiO_2@$SiW_{11}Co$ in the photoanode film shows a great advantage in enhancing the absorption of DSSC, and demonstrated the ability to conduct out holes from the valence band of TiO_2, which helps to avoid the recombination of charge carriers in the DSSC. Furthermore, a DSSC using this novel photoanode exhibited a short-circuit photocurrent density as high as 18.05 mA cm^{-2}, open-circuit photovoltage of 0.718 V, and overall light conversion efficiency as high as 6.0% under the standard AM1.5G global solar irradiation conditions. The short-circuit photocurrent density gave an excellent performance which was 64% higher than blank samples. Heteropolyacids may be new photoanode materials being used in DSSCs with high efficiency for their special physical and chemical characteristics.

Acknowledgements

This work was supported by National Natural Science Foundation of China (grant 21171044, 21371040 and 21071035), the National key Basic Research Program of China (973 Program, no. 2013CB632900) and the key Natural Science Foundation of the Heilongjiang Province, China (no. ZD201009, ZD201101 and B200907).

Notes and references

1 B. O. Regan and M. Gratzel, *Nature*, 1991, **353**, 737.
2 M. Gratzel, *Nature*, 2001, **414**, 338.
3 Y. F. Zhang, H. R. Zhang, Y. F. Wang and W. F. Zhang, *J. Phys. Chem. C*, 2008, **112**, 8553.
4 X. Wang, Y. L. Yang, P. Wang, L. Li, R. Q. Fan, W. W. Cao, B. Yang, H. Wang and J. Y. Liu, *Dalton Trans.*, 2012, **41**, 10619.
5 X. Wang, Y. L. Yang, Z. H. Jiang and R. Q. Fan, *Eur. J. Inorg. Chem.*, 2009, 3481.
6 S. H. Kang, H. S. Kim, J. Y. Kim and Y. E. Sung, *Mater. Chem. Phys.*, 2010, **124**, 422.
7 R. Asahi, T. Morikawa, T. Ohwaki, K. Aoki and Y. Taga, *Science*, 2001, **293**, 269; S. Livraghi, M. C. Paganini, E. Giamello, A. Selloni, C. D. Valentin and G. Pacchioni, *J. Am. Chem. Soc.*, 2006, **128**, 15666.
8 R. Sivakumar, J. Thomas and M. Yoon, *J. Photochem. Photobiol., C*, 2012, **13**, 277.
9 M. A. Schwegler and H. Vanbekkum, *Appl. Catal.*, 1991, **74**, 191.
10 S. Anandan, S. Pitchumani, B. Muthuraaman and P. Maruthamuthu, *Sol. Energy Mater. Sol. Cells*, 2006, **90**, 1715; S. Anandan and R. Sivakumar, *Phys. Status Solidi A*, 2009, **206**, 343.
11 S. M. Wang, L. Liu, W. L. Chen, E. B. Wang and Z. M. Su, *Dalton Trans.*, 2013, **42**, 2691.
12 X. L. Wang, H. Y. Lin, G. C. Liu, B. K. Chen and Y. F. Bi, *Chem. Res. Chin. Univ.*, 2008, **24**, 129.
13 R. H. Ma and F. P. Wang, *Chin. J. Inorg. Chem.*, 2007, **23**, 51.
14 K. Nauka and T. Kamins, *J. Electrochem. Soc.*, 1999, **146**, 292.
15 L. Jing, X. Sun, J. Shang, M. Cai, Z. Xu, Y. Du and H. Fu, *Sol. Energy Mater. Sol. Cells*, 2003, **79**, 133.
16 N. Yang, G. Q. Li, W. L. Wang, X. L. Yang and W. F. Zhang, *J. Phys. Chem. Solids*, 2011, **72**, 1319.
17 Z. Xu, J. Shang, C. Liu, C. Kang, H. Guo and Y. Du, *Mater. Sci. Eng., B*, 1999, **63**, 211.
18 A. Hiskia, A. Mylonas and E. Papaconstantinou, *Chem. Soc. Rev.*, 2001, **30**, 62.
19 M. Yoon, J. A. Chang, Y. G. Kim, J. R. Choi, K. Kim and S. J. Lee, *J. Phys. Chem. B*, 2001, **105**, 2539.
20 H. N. Tian, X. C. Yang, J. Y. Cong, R. Chen, C. Teng, J. Liu, Y. Hao, L. Wang and L. Sun, *Dyes Pigm.*, 2010, **84**, 62.
21 K. M. Lee, V. Suryanarayan and K. C. Ho, *J. Power Sources*, 2008, **185**, 1605.
22 C. He, Z. Zheng, H. Tang, L. Zhao and F. Lu, *J. Phys. Chem. C*, 2009, **113**, 10322.
23 H. Tian, L. Hu, C. Zhang, L. Mo, W. Li, J. Sheng and S. Dai, *J. Mater. Chem.*, 2012, **22**, 9123.
24 H. Xu, X. Tao, D. T. Wang, Y. Z. Zheng and J. F. Chen, *Electrochim. Acta*, 2010, **55**, 2280.

